ADVANCED FUNCTIONAL MATERIALS
www.afm-journal.de

Polymer Field-Effect Transistors Fabricated by the Sequential Gravure Printing of Polythiophene, Two Insulator Layers, and a Metal Ink Gate

By *Monika M. Voigt,* Alexander Guite, Dae-Young Chung, Rizwan U. A. Khan, Alasdair J. Campbell,* Donal D. C. Bradley, Fanshun Meng, Joachim H. G. Steinke, Steve Tierney, Iain McCulloch, Huguette Penxten, Laurence Lutsen, Olivier Douheret, Jean Manca, Ulrike Brokmann, Karin Sönnichsen, Dagmar Hülsenberg, Wolfgang Bock, Cecile Barron, Nicolas Blanckaert, Simon Springer, Joachim Grupp,* and *Alan Mosley*

The mass production technique of gravure contact printing is used to fabricate state-of-the art polymer field-effect transistors (FETs). Using plastic substrates with prepatterned indium tin oxide source and drain contacts as required for display applications, four different layers are sequentially gravure-printed: the semiconductor poly(3-hexylthiophene-2,5-diyl) (P3HT), two insulator layers, and an Ag gate. A crosslinkable insulator and an Ag ink are developed which are both printable and highly robust. Printing in ambient and using this bottom-contact/top-gate geometry, an on/off ratio of $>10^4$ and a mobility of 0.04 $cm^2\ V^{-1}\ s^{-1}$ are achieved. This rivals the best top-gate polymer FETs fabricated with these materials. Printing using low concentration, low viscosity ink formulations, and different P3HT molecular weights is demonstrated. The printing speed of 40 m min^{-1} on a flexible polymer substrate demonstrates that very high-volume, reel-to-reel production of organic electronic devices is possible.

1. Introduction

Organic electronic devices can be used in a wide range of applications.[1–5] These vary from organic light-emitting diodes (OLEDs) for mobile phones and televisions to organic field-effect transistors (OFETs) for rollable displays, wearable computers, and other portable devices such as electronic paper. Other potential applications include solar-cell photovoltaics, photodetecting and imaging systems, memory, sensors, radio frequency identification cards (RFIDs), and batteries.

A key potential advantage of organic semiconducting polymers and small molecules is their ability to be manufactured into device structures by solution processing at

[*] Dr. M. M. Voigt, Dr. A. J. Campbell, A. Guite, D.-Y. Chung, Dr. R. U. A. Khan, Prof. D. D. C. Bradley
Experimental Solid State Group and the Centre for Plastic Electronics, Department of Physics
Imperial College London, The Blackett Laboratory
South Kensington Campus, London SW7 2AZ (UK)
E-mail: m.voigt@imperial.ac.uk; alasdair.campbell@imperial.ac.uk

Dr. F. Meng,[+] Dr. J. H. G. Steinke
Department of Chemistry, Imperial College London
South Kensington Campus, London SW7 2AY (UK)

Dr. S. Tierney, Prof. I. McCulloch[++]
Merck Chemicals, Chilworth Science Park
Southampton SO16 7QD (UK)

Dr. H. Penxten, Dr. L. Lutsen, Dr. O. Douheret,[+++] Prof. J. Manca
Institute for Material Research, Hasselt University
Division IMOMEC/IMEC
Wetenscharpspark 1, 3590 Diepenbeck (Belgium)

Dr. U. Brokmann, K. Sönnichsen, Prof. D. Hülsenberg
Technische Universität Ilmenau
PO Box 100 565, 98684 Ilmenau (Germany)

W. Bock
Norbert Schläfli Maschinen
Mühletalstr. 69, 4800 Zofingen (Switzerland)

C. Barron, N. Blanckaert, Dr. S. Springer, Dr. J. Grupp
Swatch Group R&D SA – Asulab
Rue des Sors 3, 2074 Marin (Switzerland)

Dr. A. Mosley
IC Consultants Ltd, 58 Prince's Gate
Exhibition Road, London, SW7 2PG (UK)

[+] Current address: GE (China), Research Development Center Co. Ltd., 1800 Cailun Road, Zhangjang Hightech Park, Pudong District, Shanghai 201203, P. R. China

[++] Current address: Department of Chemistry, Imperial College of Science, Technology and Medicine, South Kensington, London SW7 2AY, UK

[+++] Current address: Laboratory of Chemistry for Novel Materials, Materia Nova, Avenue Nicolas Copernic 1, 7000 Mons, Belgium

DOI: 10.1002/adfm.200901597

room temperature and pressure using coating and printing techniques. Screen printing and ink-jet printing are examples of contact and noncontact printing methods, respectively.[6–16] Other techniques include pad printing in combination with doctor blading, microcontact and multitransfer printing (so-called soft lithography methods), and selective patterning by dewetting.[6,8,17–21]

An alternative technique is gravure contact printing. This is a fast and simple technique traditionally used for the mass production of newspapers, magazines, currency, postage stamps, and packaging. It has the highest throughput in comparison to other mass printing techniques reaching speeds of 60 $m^2 s^{-1}$. It can either be used as a sheet-to-sheet or a reel-to-reel process (roto-gravure).

The use of gravure for the printing of organic electronic devices is very attractive due to its very high throughput, optimal control of feature size, ability to use any substrate, ability to independently vary printing plate/ink/substrate temperature, and its ability to use a very wide range of potentially aggressive inks, solvents, and particulates. It avoids the issues of other techniques such as ink-jet printing, which includes the incompatibility of some printer heads with solvent variations, a poor control of layer thickness, pixilation of line features, and a relatively low throughput of 0.01 $m^2 s^{-1}$.[10–16]

Recent results combining gravure with other printing techniques have shown the potential of this technique. Huebler et al. demonstrated printed OFETs where gravure was combined with flexography and offset.[22] The devices had a typical on/off ratio of $10^{2.5}$, whereas the spin-coated control samples gave a higher value of $10^{3.45}$. Tobjörk et al. demonstrated successfully the printing of poly(3,4-ethylenedioxythiophene):poly(styrene sulfonate) (PEDOT:PSS) and poly(3-hexylthiophene-2,5-diyl):[6,6]-phenyl-C_{61}-butyric acid methyl ester (P3HT:PCBM) for solar cells with reverse gravure, a technique involving an additional pattern transfer drum so that the substrate is moved opposite (reverse) to the roll direction of the engraved drum.[23] Puetz et al. have produced gravure-printed indium tin oxide (ITO) layers.[24] OLEDs with gravure-printed PEDOT:PSS and light-emitting polymer layers have also been demonstrated.[25] Silver ink has also been gravure-printed for RFID aerials coupled to ring oscillators and inverters.[26–28] More recently, Tobjörk et al. and Kaihovirta et al. were able to fabricate thin-film transistors (TFTs) with roto-gravure-printed P3HT and poly(vinylpyrrolidone) (PVP) insulator layers.[29,30] No mobility values were reported, but on/off ratios were of the order of 10^2. More impressively, Yan et al. reported high-mobility n-type polymer TFTs, which they were additionally able to fabricate by gravure printing the polymer layer and dielectric layer.[31] Linked to a similarly printed P3HT p-type TFT, they were able to produce inverters. The use of this fabrication technique looks very promising.

Here we report in detail the fabrication of OFETs in which gravure contact printing is used to deposit all the principal active materials needed for organic electronic devices. Four different layers are sequentially printed: the active polymer semiconductor P3HT, two insulator layers, and an Ag ink top metal gate. The viscosity and shear behavior of P3HT inks are investigated and formulations developed for printing different P3HT molecular weights. Non-crosslinkable and crosslinkable insulator inks are developed and printed. Commercial and new Ag inks with appropriate conductivity are also successfully printed. The highest gravure print resolution features have also been achieved using glass clichés. The resultant gravure-printed top-gate/bottom-contact OFETs have a performance similar to current state-of-the art devices fabricated by small-scale methods, such as spin-coating combined with thermal metal evaporation. The use of gravure alone and a flexible plastic substrate show that these results apply to not only a sheet-to-sheet process, but also a continuous reel-to-reel process.

2. Results and Discussion

2.1. Gravure Contact Printing

The gravure contact printing process is illustrated in Figure 1i. A planar gravure cliché (printing plate) and cylindrical substrate configuration was used in this work, the alternative being a

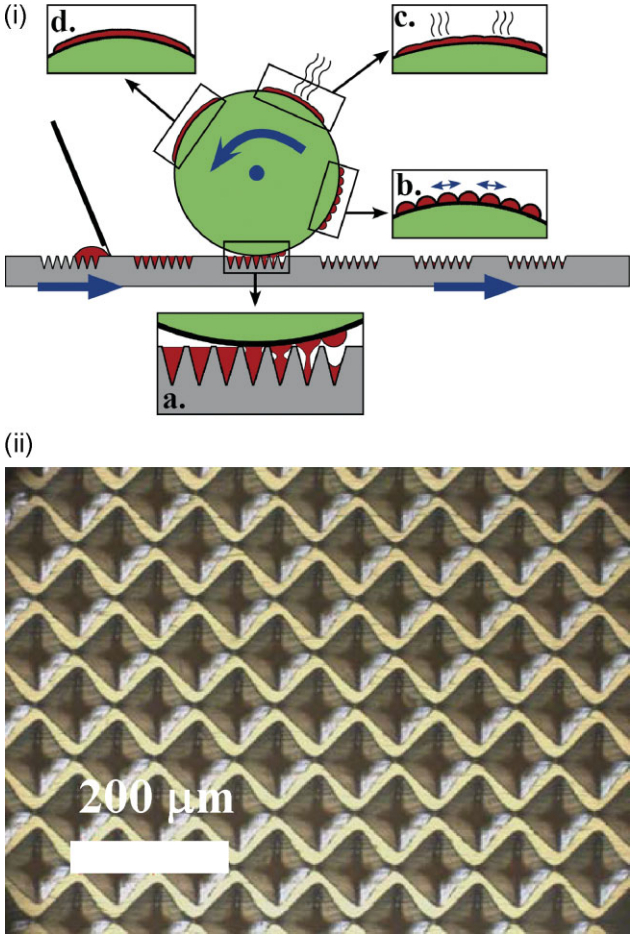

Figure 1. i) Schematic of the gravure printing process with the planar cliché used in this work (industrial R2R gravure uses a cylindrical cliché). The substrate is fixed to a cylinder which is free to rotate. The cliché moves from left to right. The doctor blade on the left of the figure scrapes ink into the cells as the cliché moves. Insets: a.) ink transfer from the cliché cells to the substrate; b.) spreading of the ink to form a uniform film; c.) solvent evaporation; and d.) deposited thin film. ii) Etched Cu cliché (110 lines/cm) showing ink cells.

cylindrical cliché and a planar substrate. The cliché consists of a chromium-plated copper plate whose surface is machined to give the print pattern. The print pattern is made up of an array of small cells (typical width 50–100 μm), which hold the ink. An example of the ink cells of an etched plate can be seen in Figure 1ii. During printing, the cliché moves from left to right in Figure 1i at a typical speed of about 1 m s^{-1}. As the cliché moves, ink deposited at one end of the cliché is scraped by the fixed doctor blade into the cells, and any surplus is removed. The substrate is attached to a rotating cylindrical drum which is synchronized with the cliché motion. The drum is pressed down onto the cliché and picks up the ink in the cells as the plate passes underneath it. For successful ink transfer, the surface energy and wetting behavior of the substrate must be more favorable to the ink than those of the cliché (Fig. 1i, inset a). Also, the shear forces, dependent on the printing speed and ink shear behavior, must allow the ink to be pulled onto the substrate. The ink droplets transferred from the cells must then flow together to form a continuous pattern (Fig. 1i, inset b). This is dependent on the substrate surface energy, ink viscosity, ink surface tension, and evaporation rate of the ink solvent(s). If this does not occur successfully, a pattern is formed consisting of separated dots mirroring the cell pattern on the cliché. The solvent then evaporates (Fig. 1i, inset c) leaving behind a layer of material in the print pattern (Fig. 1i, inset d). The same issues apply to any subsequent printed layers.

For this work flexible polyethersulphone (PES) substrates were used. As is usual for ink-jet printed organic electronic devices, these substrates had prepatterned electrodes, in this case an array of photolithographically patterned ITO source and drain contacts. A set of gravure clichés were etched with designs to print an array of transistors consisting of separate polymer semiconductor rectangles, insulator layers, and conductive ink gates.

2.2. Printing P3HT

The semiconductor P3HT was chosen as it is widely used as a model system. We investigated P3HT over a wide range of different molecular weights ($M_w = 25$ to 35 kDa as standard molecular weight (SMW) range and a 158 kDa sample as an example for a high M_W range (HMW)) using different solvents, solvent blends, and concentrations. Contact angle measurements showed that typical P3HT formulations in such solvents as *ortho*-dichlorobenzene (*o*-DCB) had a lower contact angle of 5–10° on the substrates than the clichés, hence preferentially wetting the former. The viscosity and shear behavior of P3HT formulations were also compared to reference inks from the gravure printing industry using steady-state flow measurements, involving a gradual change in stress, and continuous flow measurements, involving sudden changes in shear rate and stress. The high shear viscosity of the reference inks was in the range of 100–500 mPa s, and they showed a typical shear thinning behavior as part of their thixotropy (see Fig. 2i). High concentrations of P3HT (SMW) in chlorobenzene (CB) at room temperature showed a similar shear thinning and thixotropic behavior. The thickness and surface roughness of the printed P3HT layers for this concentration were about 600 ± 100 nm. This surface roughness is unsuitable for top-gate TFTs. Also, conductivity measurements showed that ambient impurities (oxygen and/or water) act as a p-type dopant, resulting in an undesirably high TFT off-current for films of this thickness. Generally all print formulations at high P3HT concentrations were found to produce films that were both too thick and too uneven.

To reduce film thickness and surface roughness, low concentrations of P3HT (SMW) in *o*-DCB, 1,2,3,4-tetrahydronapthalene (THN), and other solvents and solvent blends were

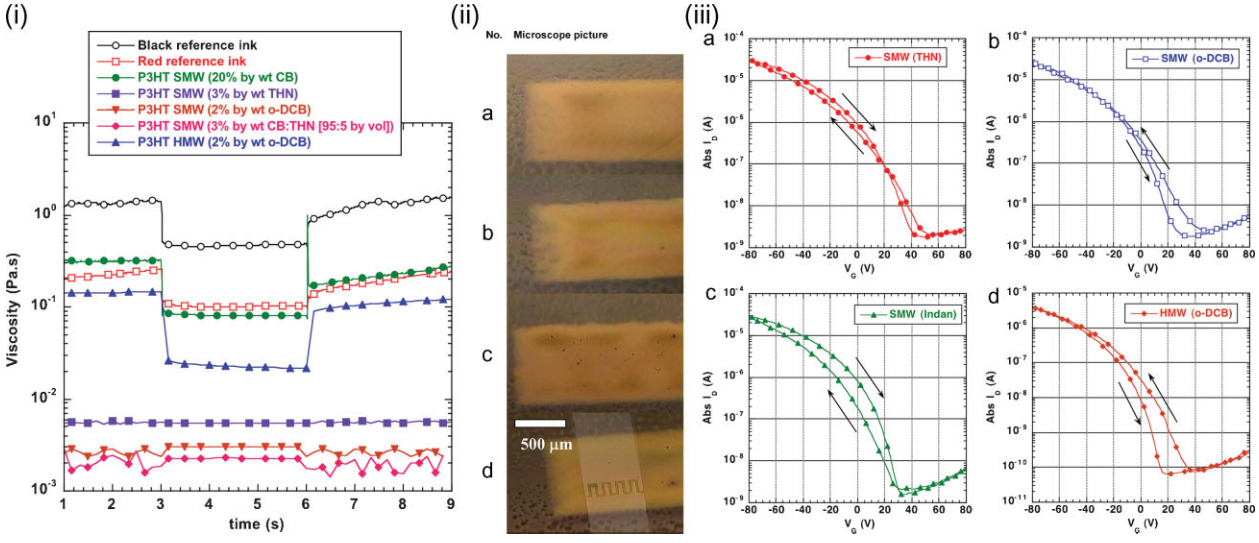

Figure 2. i) Viscosity versus time shear flow measurements of different inks. Between 3–6 s, shear rate was 1200 s^{-1}. Before 3 s and after 6 s, shear rate was 10 or 50 s^{-1}. Inks are commercial black and red reference inks; SMW P3HT formulations of 20% by wt in CB, 3% by wt in THN, 2% by wt in *o*-DCB, and 3% by wt in CB:THN (ratio by volume (vol) 95:5); HMW P3HT formulation of 2% by wt in *o*-DCB. ii) Gravure-printed films of P3HT. SMW (3% by wt) in THN (ii.a), *o*-DCB (ii.b), and indan (ii.c); and HMW (2% by wt) in *o*-DCB (ii.d). Thickness (RMS roughness) is 100 ± 10 (ii.a,b), 100 ± 15 (ii.c), and 95 ± 15 (ii.d) nm. iii) Transfer characteristics (drain voltage, $V_D = -30$ V) for TFTs with gravure-printed P3HT: iii.a–c) printed SMW P3HT (3–4% by wt) in THN (iii.a), *o*-DCB (iii.b), and indan (iii.c) /spin-coated PHEMA/evaporated Al gate, and printed HMW P3HT (2% by wt) in *o*-DCB/spin-coated PMMA/evaporated Al gate (iii.d).

investigated. These follow Newtonian behavior and are at a much lower viscosity of 1–10 mPa s (Fig. 2i). Typical printed films for low concentrations of P3HT (SMW) in THN, *o*-DCB, and indan are shown in Figure 2ii.a–c. These have a thickness and surface roughness of about 100 ± 10 nm. This clearly shows that low viscosity formulations (atypical in standard gravure), with values similar to those used in other techniques, such as ink-jet and standard molecular weight polymer semiconductors can be successfully printed using gravure. These also involve low concentration formulations (3–4% by weight (wt)), again similar to those used in ink-jet printing and spin-coating.

To explore the formulation behavior further a HMW batch of P3HT was also investigated. At low concentrations in *o*-DCB, the shear thinning and thixotropic behavior were more similar to the standard inks (see Fig. 2i). Typical printed films are shown in Figure 2ii.d and have a thickness and surface roughness of about 95 ± 15 nm. As expected high molecular weight materials can be printed at slightly lower concentrations, with the higher viscosity and non-Newtonian behavior exhibiting no detrimental effect on film quality.

In general, the coverage and smoothness of the printed film increased as the boiling point of the solvent increased, presumably due to the slower evaporation rate allowing the printed layer time to spread into a continuous film (figuratively illustrated in Fig. 1i, insets b–d). High concentrations (>10% by wt) tended to lead to unacceptably thick and rough films, while very low concentrations (1% by wt) tended to lead to poor coverage, with surface features, and holes aligning in the print direction.

Figure 2iii shows typical transfer characteristics of FETs fabricated using films similar to those shown in Figure 2ii. These were fabricated by printing on the prepatterned ITO source and drain contacts (shown clearly underneath the P3HT film in Fig. 2ii.d) and using spin-coated insulator layers of either poly(2-hydroxyethyl methacrylate) (PHEMA) (for SMW P3HT devices) or poly(methyl methacrylate) (PMMA) (for HMW P3HT devices) and an evaporated Al top gate. The SMW P3HT devices have a very similar saturation mobility of 0.008–0.005 $cm^2 V^{-1} s^{-1}$ and an on/off ratio of $10^{4.2}$–$10^{4.3}$. This should be compared to control devices of the same structure fabricated with spin-coated P3HT and prepared in a nitrogen filled glovebox, which have a saturation mobility of 0.005 $cm^2 V^{-1} s^{-1}$ and an on/off ratio of $10^{4.4}$–$10^{4.9}$. The devices with printed semiconductors therefore possess a mobility in a similar range to that of the spin-coated devices, the slightly lower on/off ratio being ascribed to printing the P3HT in ambient. Although atomic force microscopy (AFM) characterization indicated changes in surface structure depending on whether the P3HT had been printed from *o*-DCB, indan, or THN, no correlation could be found between this and device performance, unlike previous results for bottom-gate P3HT FETs.[32–35] The HMW P3HT devices have a saturation mobility of 0.007–0.003 $cm^2 V^{-1} s^{-1}$ and an on/off ratio of $10^{4.8}$, which are in a similar range to those of the SMW printed and spin-coated P3HT devices.[36]

2.3. Printing Dielectrics

A wide range of insulators with different solvents were gravure-printed on P3HT. These included PVP, poly(vinyl alcohol) (PVA), PMMA, and PHEMA.[37–41] The requirement criteria for printing

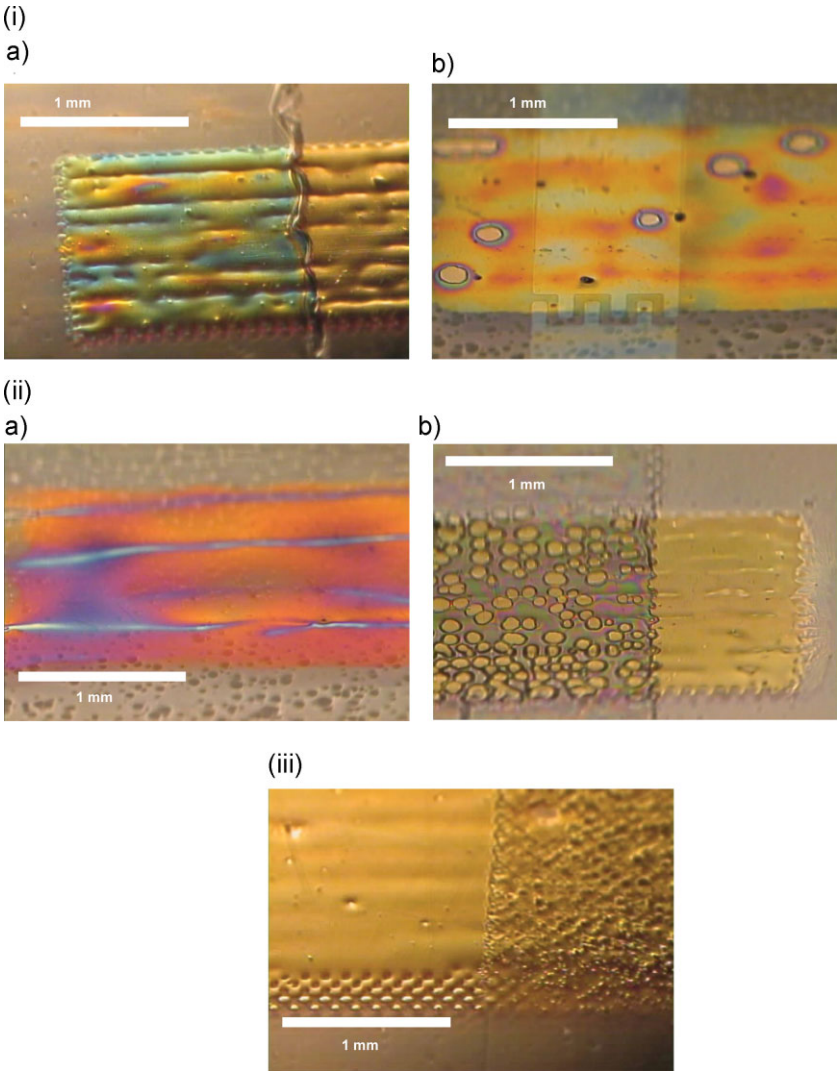

Figure 3. Gravure printing behavior of insulators. i) Wetting behavior of PHEMA: i.a) on the left side printed PHEMA (10% by wt in isopropanol (IPA)) on printed P3HT (20% by wt in CB); and i.b) printed XL-PHEMA (8% by wt in TFE) showing signs of dewetting on printed P3HT (3% by wt in THN). ii) Wetting behavior of PMMA: ii.a) printed PMMA (5% by wt in MEK) on printed P3HT (3% by wt in THN); and ii.b) on the left side printed PMMA (10% by wt in MEK) dewetting on printed P3HT (20% by wt in CB). iii) Example of printing the insulator from a solvent that is not orthogonal to P3HT (in the case CB). On the right side of the P3HT rectangle the printed insulator ink has dissolved the P3HT layer underneath.

the insulator layer are more demanding because it must not only successfully print on P3HT, but also on the ITO and the substrate surface. It was found that the same insulator would change its wetting behavior on P3HT or the substrate depending on the insulator solvent choice, or semiconductor solvent choice if not completely removed (prior to printing the subsequent layer) (Fig. 3i,ii). Poor solvent choice for the insulator could also lead to dissolution of the underlying P3HT layer (see Fig. 3iii). It was also found that certain insulators could dewet from P3HT minutes to days later if the solvent used to print the P3HT layer underneath was not removed carefully.

PMMA and PHEMA gave very good, high quality printed films and have an orthogonal solubility to P3HT and the conductive metal ink formulations. They also show good performance in fully spin-coated FETs and have a high breakdown voltage (>120 V for 500 nm thick layers). Relative dielectric permittivities ε_r were measured as 3.2 and 7.8 respectively. PMMA was printed using a wide range of molecular weights ($M_w = 30$–100 kDa) and solvents (acetone, butanone (methyl ethyl ketone (MEK))) at low concentrations. PHEMA was also printed using a wide range of molecular weights ($M_w = 31$–80 kDa). It is more hydrophilic and can be printed using water/alcohol or solely alcohol-based solvents such as 2,2,2-trifluoroethanol (TFE). A crosslinkable version of PHEMA (XL-PHEMA) was additionally developed to improve environmental stability and structural robustness and to enhance chemical stability to minimize potential solubility issues arising from further printed or deposited layers. XL-PHEMA was successfully printed in TFE, with added crosslinking agent, and has a similar printing behavior, thickness and roughness to PHEMA. The printing was followed by a heating cycle to allow chemical crosslinking occur. The dielectric relative permittivity was measured and is 5.3. The most successful PMMA, PHEMA, and XL-PHEMA formulations were found to exhibit Newtonian behavior and have a viscosity in the 10 mPa s range. This is again much lower than the reference inks, and in the same range as that found for the most successful P3HT formulations.

The three printed insulators all gave layers of about 250 nm thickness. This is too thin for FETs, leading to high leakage currents and a high probability of breakdown. To avoid this and to improve surface roughness, XL-PHEMA formulations were adjusted so that they could be successfully printed on top of printed PMMA, PHEMA, or XL-PHEMA layers. The resultant printed two insulator layer structures were found to have a thickness of around 0.5 μm and a maximum surface roughness of ±50 nm. The capacitance per unit area was found to be equal to a simple series combination. Two insulator layers were also found to give a higher resistance to voltage breakdown.

2.4. Printing Metal Gates and Drive Lines

Finally, Ag metal inks were investigated for the conducting top gate. Both synthesized Ag inks, consisting of dispersed nanocolloidal particles (20–50 nm) in α-terpineol, and a commercially available Cabot silver ink in solution were successfully gravure-printed (see Fig. 4i–iii). Again the formulations were found to exhibit Newtonian behavior with a viscosity of about 16 mPa s, which is consistent with the Cabot ink being specifically designed

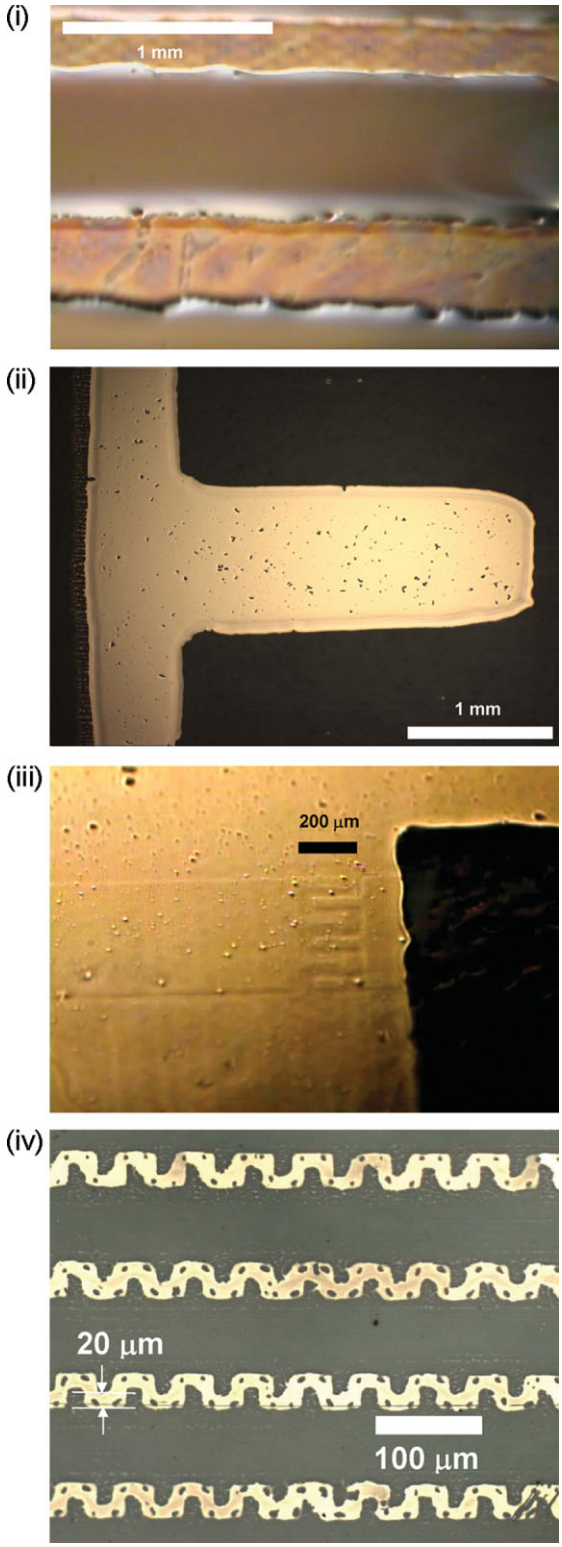

Figure 4. Gravure printing behavior of metal inks. i) Printed Cabot ink on printed PMMA (10% by wt in acetone). ii) Synthesized silver ink printed on PES substrate. iii) Printed silver ink on top of a double layer of printed and crosslinked XL-PHEMA on top of printed P3HT on top of the pre-etched source–drain structure (this can be seen underneath). iv) Example of a silver ink gravure-printed with a glass cliché.

as a low-viscosity formulation for ink-jet printing. Both the synthesized inks and the Cabot ink showed good film forming properties with a typical layer thickness of 120 nm and a surface roughness of ± 10 nm. After the appropriate annealing step between 120 and 150 °C, sheet resistances of 0.4 (synthesized, 30% by wt in α-terpineol) and 0.9 (Cabot) Ω square^{-1} were achieved. Drive lines of 1 mm width and 10 cm length were achieved. However, the Cabot ink was found to dissolve PHEMA and dewet on XL-PHEMA. The as-synthesized nanocolloidal Ag ink showed very good wetting and printing behavior. It does not dissolve PHEMA, nor is it dissolved by the highly aggressive solvents contained in commercially used encapsulation material formulations developed for use with Si-based FETs.

To explore the resolution of gravure, new experimental, photolithographically patterned glass clichés with reduced cell sizes were also tested with the Ag metal ink formulations. Manufactured using a photosensitive glass, cells of a width of 10 μm and a depth of <10 μm were achieved.[42,43] Figure 4iv shows lines of Ag Cabot ink printed using this type of cliché. The meander structure has a width of 20 μm and an internal feature separation of 20 μm. Although not used with the FETs fabricated here as they require further development, this does show the potential of gravure to print structures well below the dimensions achievable with current clichés.

2.5. Printed P3HT, Two Dielectric Layers, and Ag Ink Gate FETs

Finally, FETs were fabricated using gravure-printed P3HT, a first insulator layer of gravure-printed PMMA, PHEMA, or XL-PHEMA, a second insulator layer of gravure-printed XL-PHEMA, and a final layer of gravure-printed synthesized Ag ink for the gate (Fig. 5i). No working devices with PMMA as the first insulator layer were achieved. This is believed to be due to the low robustness of the PMMA layer to this contact printing process and the thermal annealing steps being higher than its glass transition temperature. Devices with XL-PHEMA as the first insulator layer had a saturation mobility of 0.002 cm^2 V^{-1} s^{-1} and on/off ratio of 10^1–10^2. This reflects the values found for devices using spin-coated XL-PHEMA as the insulator layer, which had mobility values about an order of magnitude below that of similar devices using PHEMA. The lower performance using XL-PHEMA is believed to be due to chemical reactions with the P3HT at the semiconductor–insulator boundary due to the crosslinking process. Devices with PHEMA as the first insulator layer consistently showed good transistor performance, a range of devices being printed with mobilities of 0.001–0.01 cm^2 V^{-1} s^{-1} and on/off ratios of 10^2–10^4.

The best transistor performance was achieved for P3HT/PHEMA/XL-PHEMA/Ag ink (Fig. 5ii). This structure yielded an on/off ratio of $10^{3.9}$–$10^{4.6}$ with a saturation mobility of 0.03–0.04 cm^2 V^{-1} s^{-1}. Gate leakage currents were similar to fully spin-coated reference devices with a single insulator layer of equivalent thickness (i.e., 500 nm of PHEMA). Intriguingly the mobility values are higher than those of printed P3HT devices with spin-coated PHEMA. This suggests that the differences in insulator solvent and/or the temperature cycles used to anneal or crosslink the insulator and Ag ink layers lead to much better P3HT ordering and crystallinity at the semiconductor/insulator interface. The best top-gate structures processed in nitrogen using P3HT and spin-coated insulators have been reported to reach mobilities of 0.02–0.05 cm^2 V^{-1} s^{-1} and on/off ratios of 10^2–10^3.[5,23,33–36,38–39,41,44,45] The gravure-printed devices reported here have therefore reached the mobility and exceeded the on/off ratio of state-of-the-art devices prepared by spin-coating. The values for the four-gravure-printed layer devices (printed P3HT/dielectric/dielectric/Ag gate) reported here compare very favorably with those reported previously for the two-gravure-printed layer devices (printed P3HT/dielectric), falling in the same mobility

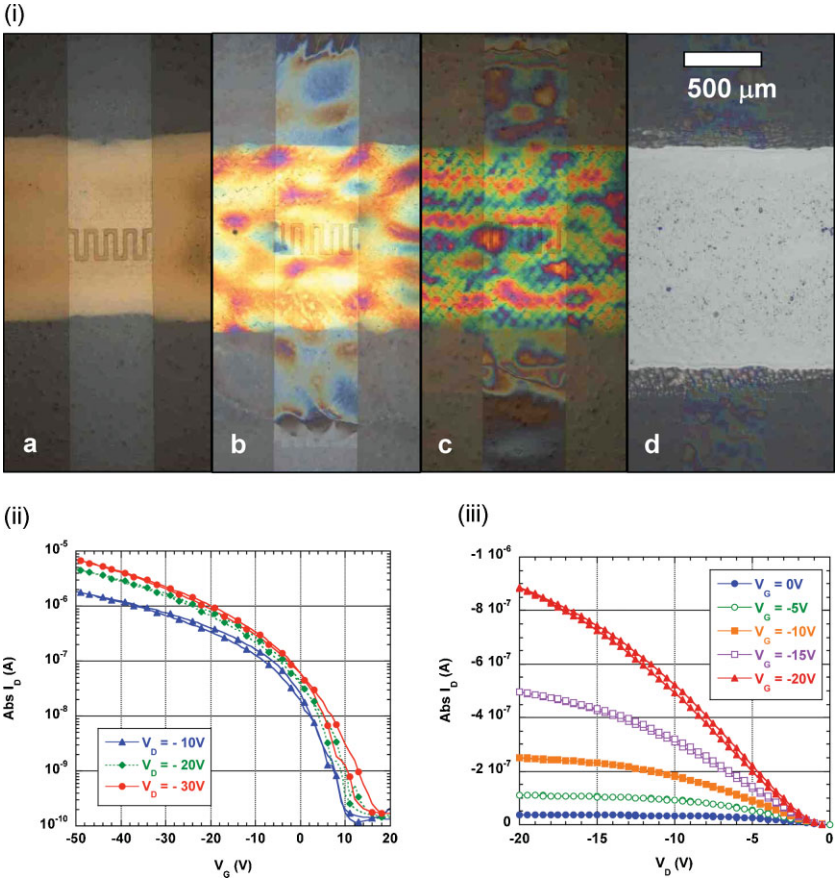

Figure 5. i) Sequential gravure printing of the transistor: P3HT (3% by wt in Indan) (i.a); after the addition of PHEMA (i.b), of crosslinked XL-PHEMA (i.c), and of Ag ink gate (i.d). ii) Transfer (ii.a) and output (ii.b) characteristics of a fully printed transistor consisting of P3HT (3% by wt in indan)/PHEMA (8% by wt in TFE)/XL-PHEMA (8% by wt in TFE)/30% Ag ink.

range of 0.02–0.1 $cm^2\ V^{-1}\ s^{-1}$ and exceeding the on/off ratio of 10^2–10^3.[31]

3. Conclusions

In conclusion, we have therefore demonstrated that it is possible to gravure-print high performance, state-of-the-art polymer FETs. The method used here is immediately applicable to a sheet-to-sheet production process, but the use of flexible substrates positioned on a curved holder shows that it is also compatible with a reel-to-reel production process. The low-concentration, low-viscosity formulations using high boiling point solvents should be transferable to other semiconducting polymers with a similar molecular weight range. Shifting to polymers which are not doped by oxygen should resolve the issue of printing in ambient.[46] Developing "Xtreme" machined, laser, or photopatterned copper or glass clichés with reduced pore size and line width will allow the source and drain to be printed with channel lengths of $< 50\ \mu m$. Using source and drain materials, such as PEDOT:PSS or Au metal inks, should lower contact resistance. This will allow bottom-gate structures to be used with self-assembled monolayers to maximize material performance.[38,39,46,47] The ability to print blend films of n- and p-type organic semiconductors and light-emitting polymers shows that gravure contact printing can be used to manufacture all the essential elements of organic electronics. The ability to use this very high-volume technique should usher in a whole range of cheap, large area devices and structures, allowing this technology to finally reach its full potential.

4. Experimental

P3HT in five different molecular weights ($M_w = 25\ 300$, 32 000, 32 500, 34 500, 158 000 Da, PS standard equivalent, measured by gel permeation chromatography (GPC)) and polydispersities in the range of 1.8 to 3 was used after purification. All solvents were obtained from Aldrich. P3HT solutions (1–20 wt%) were stirred with a magnetic stirrer overnight at room temperature or 50 °C (high boiling point solvents) and then filtered before printing. PMMA, low molecular weight PHEMA ($M_n = 16$ kDa) and other insulators were obtained from Aldrich. PHEMA with a range of molecular weights ($M_n = 17$–64 kDa) and narrow molecular weight distributions were synthesized via ATRP at Imperial. Insulators were printed at concentrations of 5–20 wt%. To make XL-PHEMA, PHEMA was blended with an aminal/acetal crosslinker poly(melamine-*co*-formaldehyde) (PMF; $M_n \approx 432$/84 wt%) in *n*-butanol, isopropanol, or trifluoroethanol at concentrations up to 40% by volume. For the gate, silver ink from Cabot and an in-house developed nanocolloid silver ink were used. The synthesized Ag ink was formulated at concentrations of 20–30 wt%.

A Labratester 1 test printer from Schläfli-Maschinen (sheet-to-sheet design) was used to print all layers. The standard printing speed was 40 m min^{-1}. Copper clichés were provided by Schläfli-Maschinen with machined cells at line densities from 40 to 210 lines/cm. Cells were pyramidal structures of about 20 μm in width and length and 25 μm in depth. The semiconductor cliché was designed to produce 1 mm × 2 mm rectangles. The gate cliché had 0.5 mm wide drive lines connected to 0.8 mm × 3 mm rectangular gates. The designs were deliberately large to reduce alignment problems. PES substrates (10 cm × 10 cm) covered in ITO were pre-etched to produce channel lengths of 30 and 50 μm and a channel width of 1.3 mm. Unetched PES, polyethylene (PE), and poly(ethylene naphthalate) (PEN) substrates were also used. Spin-coated control devices and partially printed P3HT devices were also manufactured. The spin-coated devices have been made using 3% by wt P3HT in CB at 2000 rpm for 1 min. Spin-coated dielectrics were 7% by wt PHEMA in IPA at 2500 rpm for 1 min, 8% XL-PHEMA in TFE at 4000 rpm for 1 min, and 5% PMMA in MEK at 2000 rpm for 1 min. Fully printed devices were manufactured at Imperial College Physics and Asulab.

Layer thickness was measured with a Dektak^3 Profilometer from Veeco Metrology Group and α-step 200 from Tencor Instruments. The surface investigations and examination of the wetting behavior were studied using a Zeiss Axioplan microscope with attached digital camera or the digital camera from the Dektak. Capacitance measurements of the insulators were conducted between 10 and 10^6 Hz using a Schlumberger Solartron 1260 Impedance Analyzer.

FET characteristics were measured using an Agilent 4156C semiconductor parameter analyzer. Saturation mobility was calculated from the saturation regime transfer characteristics at $V_D = -30\ V = (V_G - V_T)$ using $\partial(I_D)^{1/2}/\partial V_G = (\mu_{SAT})^{1/2}\ (C_i\ W/2L)^{1/2}$. V_T was taken as the intercept at $I_D = 0$ of a linear fit to $(I_D)^{1/2}$ versus V_G (where V_G, V_T, I_D, μ_{SAT}, C_i, W, and L represent the gate voltage, threshold voltage, drain current, saturation mobility, insulator capacitance per unit area, channel width, and channel length, respectively).

Rheology and wetting measurements were carried out using a TA instruments AR-G2 rheometer and a Dataphysics OCA15+ Optical Contact angle Measurement System, respectively.

Acknowledgements

The authors thank the European Commission for funding this work (Contact Printing of Electronics and Opto-Electronics/FP6/511562). The authors also thank the UK EPSRC for funding A. Guite. Further we would like to thank Jingsong Huang and Feng Yan for contributions to the project and valuable discussions, Norbert Schläfli Maschinen, Switzerland, for the delivery of printing plates and valuable information on gravure printing and Jenny Nelson for useful discussions regarding the manuscript.

Received: August 25, 2009
Published online: December 16, 2009

[1] D. J. Gundlach, *Nat. Mater.* **2007**, *6*, 173.
[2] H. Klauk, *Nat. Mater.* **2007**, *6*, 397.
[3] M. Berggren, D. Nilsson, N. D. Robinson, *Nat. Mater.* **2007**, *6*, 3.
[4] S. R. Forrest, *Nature* **2004**, *428*, 911.
[5] H. Sirringhaus, N. Tessler, R. H. Friend, *Science* **1998**, *280*, 1741.
[6] S. K. Park, Y. H. Kim, J. I. Han, D. G. Moon, W. K. Kim, M. G. Kwak, *Synth. Met.* **2003**, *139*, 377.
[7] D. Kim, S. Jeong, B. K. Park, J. Moon, *Appl. Phys. Lett.* **2006**, *89*, 264101.
[8] A. Knobloch, A. Manuelli, A. Bernds, W. Clemens, *J. Appl. Phys.* **2004**, *96*, 2286.
[9] T. Kraus, L. Malaquin, H. Schmid, W. Riess, N. D. Spencer, H. Wolf, *Nat. Nanotechnol.* **2007**, *2*, 570.
[10] S. H. Ko, J. Chung, H. Pan, C. P. Gigoropoulos, D. Poulikakos, *Sens. Actuators A* **2007**, *134*, 161.
[11] M. M. Ling, Z. Bao, *Chem. Mater.* **2004**, *16*, 4824.
[12] Y. Y. Noh, N. Zhao, M. Caironi, H. Sirringhaus, *Nat. Nanotechnol.* **2007**, *2*, 784.
[13] K. E. Paul, W. S. Wong, S. E. Ready, R. A. Street, *Appl. Phys. Lett.* **2003**, *83*, 2070.
[14] S. P. Speakman, G. G. Rozenberg, K. J. Clay, W. I. Milne, A. Ille, I. A. Gardner, E. Bresler, J. H. G. Steinke, *Org. Electron.* **2001**, *2*, 65.
[15] B. J. De Gans, P. C. Duineveld, U. S. Schubert, *Adv. Mater.* **2004**, *16*, 203.
[16] J. Zhang, P. Brazis, A. R. Chowdhuri, J. Szczech, D. Gamota, *Mater. Res. Soc. Symp. Proc.* **2002**, *725*, P6.3.1-6.
[17] K. Bock, *Proc. IEEE* **2005**, *9*, 1400.
[18] M. L. Chabinyc, W. S. Wong, A. Salleo, K. E. Paul, R. A. Street, *Appl. Phys. Lett.* **2002**, *81*, 4260.
[19] M. Chason, P. W. Brazis, J. Zhang, K. Kalyanasundaram, D. R. Gamota, *Proc. IEEE* **2005**, *93*, 1348.

[20] D. R. Hines, V. W. Ballarato, E. D. Williams, Y. Shao, S. A. Solin, *J. Appl. Phys.* **2007**, *101*, 024503.
[21] H. Katz, *Chem. Mater.* **2004**, *16*, 4748.
[22] A. C. Huebler, F. Doetz, H. Kempa, H. E. Katz, M. Bartzsch, N. Brandt, I. Hennig, U. Fuegmann, S. Vaidyanathan, J. Granstrom, S. Liu, A. Sydorenko, T. Zillger, G. Schmidt, K. Preissler, E. Reichmanis, P. Eckerle, F. Richter, T. Fischer, U. Hahn, *Org. Electron.* **2007**, *8*, 480.
[23] D. Tobjörk, H. Aarnio, T. Mäkelä, R. Österbacka, *Mater. Res. Soc. Symp. Proc.* **2008**, 1091-AA05-45.
[24] J. Puetz, M. A. Aegerter, *Thin Solid Films* **2008**, *516*, 4495.
[25] M. Tuomikoski, R. Suhonen, M. Välimäki, T. Maaninen, M. Sauer, P. Rogin, M. Mennig, S. Heusing, J. Puetz, M. A. Aergerter, *Proc. SPIE-Int. Soc. Opt. Eng.* **2006**, *61921*, 619204.
[26] M. Bartzsch, H. Kempa, M. Otto, A. Hübler, D. Zielke, *Org. Electron.* **2007**, *8*, 431.
[27] M. Pudas, N. Halonen, P. Granat, J. Vähäkangas, *Prog. Org. Coat.* **2005**, *54*, 310.
[28] M. Pudas, J. Hagberg, S. Leppävuori, *Prog. Org. Coat.* **2004**, *49*, 324.
[29] D. Tobjörk, N. J. Kaihovirta, T. Mäkelä, F. S. Petterson, R. Österbacka, *Org. Electron.* **2008**, *9*, 931.
[30] N. J. Kaihovirta, D. Tobjörk, T. Mäkelä, R. Österbacka, *Adv. Eng. Mater.* **2008**, *10*, 640.
[31] H. Yan, Z. Chen, Y. Zheng, C. Newman, J. R. Quinn, F. Dötz, M. Kastler, A. Facchetti, *Nature* **2009**, *457*, 679.
[32] J. F. Chang, B. Sun, D. W. Breiby, M. N. Nielsen, T. I. Siling, M. Giles, I. McCulloch, H. Sirringhaus, *Chem. Mater.* **2004**, *16*, 4772.
[33] R. J. Kline, M. D. McGehee, E. N. Kadnikova, J. Liu, J. M. J. Fréchet, M. F. Toney, *Macromolecules* **2005**, *38*, 3312.
[34] L. A. Majewski, J. W. Kingsley, C. Balocco, A. M. Song, *Appl. Phys. Lett.* **2006**, *88*, 222108.
[35] H. Yang, T. J. Shin, L. Yang, K. Cho, C. Y. Ryu, Z. Bao, *Adv. Funct. Mater.* **2005**, *15*, 671.
[36] A. Zen, J. Pflaum, S. Hirschmann, W. Zhuang, F. Jaiser, U. Asawapirom, J. P. Rabe, U. Scherf, D. Neher, *Adv. Funct. Mater.* **2004**, *14*, 757.
[37] A. Facchetti, M.-H. Yoon, T. Marks, *Adv. Mater.* **2005**, *17*, 1705.
[38] H. Sirringhaus, *Adv. Mater.* **2005**, *17*, 2411.
[39] J. Veres, S. Ogier, G. Lloyd, D. de Leeuw, *Chem. Mater.* **2004**, *16*, 4543.
[40] H. Kang, J. Park, H. H. Lee, *Adv. Mater.* **2006**, *18*, 1603.
[41] J. Park, S. Y. Park, S.-O. Shim, H. Kang, H. H. Lee, *Appl. Phys. Lett.* **2004**, *85*, 3283.
[42] D. Hülsenberg, A. Harnisch, A. Bismarck, *Microstructuring of Glasses*, Springer Series in Material Science, Springer, Berlin **2008**.
[43] U. Brokmann, K. Sönnichsen, D. Hülsenberg, *Microsyst. Technol.* **2008**, *14*, 1635.
[44] J. Ficker, A. Ullmann, W. Fix, H. Rost, W. Clemens, *J. Appl. Phys.* **2003**, *94*, 2638.
[45] H. G. O. Sandberg, T. G. Bäcklund, R. Österbacka, M. Shkunov, D. Sparrowe, I. McCulloch, H. Stubb, *Org. Electron.* **2005**, *6*, 142.
[46] I. McCulloch, M. Heeney, C. Bailey, K. Genevicius, I. Macdonald, M. Shkunov, D. Sparrowe, S. Tierney, R. Wagner, W. Zhang, M. L. Chabinyc, R. J. Kline, M. D. McGehee, M. F. Toney, *Nat. Mater.* **2006**, *5*, 328.
[47] D. M. Russell, T. Kugler, C. J. Newsome, S. P. Li, M. Ishida, T. Shimoda, *Synth. Met.* **2006**, *156*, 769.